European Journal of Computational Mechanics, 2013
Vol. 22, Nos. 2–4, 209–227, http://dx.doi.org/10.1080/17797179.2013.820896

New topological approach for the modelling of mecatronic systems: application for piezoelectric structures

M. Miladi Chaabane[a,b]*, R. Plateaux[b], J.-Y. Choley[b], C. Karra[a], A. Riviere[b]
M. Haddar[a]

[a]*Mechanical, Modeling and Manufacturing Unit, National Engineering School of Sfax (ENIS), BP 1173 – 3038, Sfax, Tunisia;* [b]*Laboratory of Engineering of the Mechanical Structures and Materials, High Institute of Mechanic of Paris (SUPMECA), 3, rue Fernand Hainaut, 93407, Saint-Ouen, Cedex, France*

In this study, a new topological approach for the modelling of mecatronic systems is presented. This approach offers the opportunity to separate the behaviour laws (physics) and the interconnection laws (topology) at local level. Then, it can be used as a unification basis for the modelling of the different fields of Mecatronics. This approach is based on the notion of topological collections and transformations and applied using the MGS language (Modelling of General Systems). The emphasis is placed on the application of this approach to the piezoelectric structures (Multi layer piezoelectric stack and piezoelectric truss structure). To validate this approach, simulation results are presented and compared with those obtained by the finite element analysis ANSYS software.

Keywords: transformations; topological collections; KBR topological graph; MGS language; piezoelectric structure

1. Introduction

Since the 1990s, the term mecatronic has spread worldwide in a remarkable way with numerous proposed definitions (the definition of the Mecatronic International newspaper in 1991, the definition of the IFAC technical Committee on Mecatronic Systems in 2000, the definition of the French Standard Organisation NF E01–010 in 2010…). The definitions of mecatronics differ in their expressions, but they all meet on a common objective to achieve manufacturing of systems that highlight the multidisciplinary aspect: mechanics, electronics, computer sciences and automation. Obviously, all the above mentioned disciplines are similar in their topology. In fact, all mecatronic systems could be decomposed in subsystems that belong to different fields of mecatronics: Each field can be characterised by its topological structure and behavioural laws (Björke, 1995; Plateaux, Penas, Rivière, & Choley, 2007).

Kron (1942) was the pioneer as well in the use of tensor analysis for electrical networks as in their generalisation to the electromechanical systems using the diakoptics method (Kron, 1963). In this method a physical system is dissected into an appropriate number of small subdivisions, each of which is analysed and solved separately. The partial solutions are then interconnected step by step until a solution for the entire

*Corresponding author. Email: mariam.mi@hotmail.fr

system is achieved. In 1966, Branin (1966) who relied on Kron's work, which was validated mathematically by Roth (1955) on the electrical networks and machines, was able to use the same topological structure to describe the physical quantities of multi-physical systems. The generic modelling approach consists in representing the system by a topological structure (linear or planar graph). This structure connects the various topological entities (nodes, branches and meshes) of the graph. To the first topological structure are associated two other topological structures known as chain complexes and co-chain complexes together with the physical parameters that govern the behaviour of the studied system. Later, Björke (1995) resumed these works and extended them to the manufacturing systems integrating the problems of control, planning and cost.

Several researchers have applied a topological approach for the modelling of mechanical systems. For example: Shai (2001a, 2001b, 2001c) developed a Combinatorial Representations (CR) based on graph and matroid theory and applied it to different engineering fields in particular to the analysis of trusses, Egli (2000) described a framework for the specification and manipulation of models of systems (mass-spring systems network, fluid particles …) using chain models, and Tonti (2003) described physical laws by algebraic topology using cell complexes.

Therefore, in this study, we are interested in applying a topological approach for the modelling of mecatronic systems. This study would make it possible to separate the topology and the physics of the studied system in order to have generic local models allowing the optimisation of the system behaviour according to the whole system. This study is a continuation and extension of the work directed by Plateaux as part of his thesis (Plateaux, 2011) entitled "Continuity and coherence of mecatronic systems modelling based on a topological approach" and presented in 2011. Plateaux, primarily relying on the works of Kron (1942, 1963), Roth (1955) and Branin (1966) previously introduced, applied the KBR topological graph (named KBR in honour of its creators) for the modelling of mecatronic systems. He used the MODELICA language that enabled him to apply this graph (MODELICA, 2013). In fact, MODELICA language allows to take a specific type of topological connexions into account and uses the concepts of flow and potential and consequently respect the Kirchhoff's laws. On the other hand, its topological nature is limited to 0 and 1 complexes and the access to higher dimensions can be done only via transformations to 0-simplexes. Therefore, it associates the topology and the behaviour into the same model that limits the generalisation of the studied system. In our study, however, we used the MGS (Modelling of General Systems) language that proposes a unified view on several computational mechanisms initially inspired by biological processes. MGS is a research project, developed in the IBISC (Laboratory for Computer Science, Integrative Biology and Complex Systems) of the University of Evry (France). It is especially devoted to the simulation of biological systems whose state space structure evolves dynamically in time (The MGS home page, 2013; Giavitto, Godin, Michel, & Prusinkiewicz, 2002; Spicher & Michel, 2007). The basic data structure of MGS is topological collections that are composed of elements of various dimensions called topological cells organised according to a certain topology and associated with values (Cohen, 2004; Spicher, 2006).

The main objective of this study is to develop a general topological approach as a support for the modelling of mechatronic systems. This approach is based on the KBR topological graph and applied using topological collections in order to present a topological structure (interconnection law) of a mecatronic system and transformations in order to specify its local behaviour laws. The emphasis is put on the application of this method to piezoelectric structures.

The remainder of this study is organised as follows: Section 2 sheds light on the modelling of mecatronic systems using the KBR topological graph and its application via the topological collections and transformations. Then, section 3 is dedicated to the application of this topological approach to the case of piezoelectric structure. Two particular cases are treated: multi layer piezoelectric stack and piezoelectric truss structure. The numerical results obtained by the MGS language are presented and compared with those obtained by the finite element analysis ANSYS software. Our conclusions are drawn in Section 4.

2. Topological modelling

2.1. The KBR topological graph

In 2007, Plateaux proposed a general geometrical and topological structure for the modelling of complex systems (Plateaux et al., 2007). This modelling is based on the integration of the topological algebra and geometric algebra and applied them using the KBR topological graph.

To determine the KBR topological graph, we present the system as a cellular complex which is an abstract topological structure that generalises to higher dimension the notion of graph. Then, we extract the complexes of chain and co-chain of these topological structures to which the physical and geometrical variables of interest are associated. Figure 1 shows an example of a cellular complex and its chain complex made up of five cells of dimension 0 representing the nodes, six cells of dimension 1 representing the branches and two cells of dimension two representing the faces.

Figure 2 shows the KBR topological graph. In fact, we can go left again to bring up the surfaces, volumes ... according to the specifications of the problem. In this graph

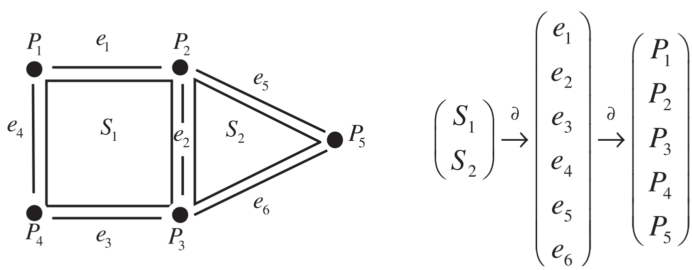

Figure 1. Example of a cellular complex and its chain complex linked by a boundary relationship.

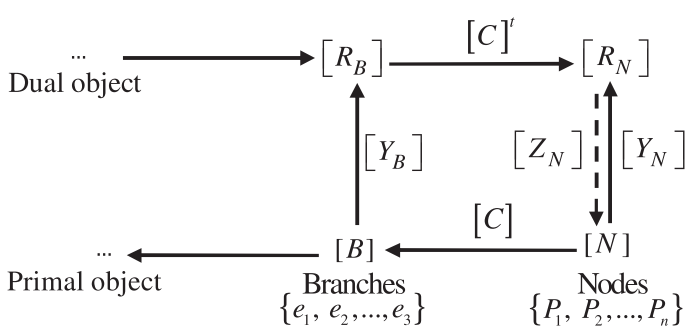

Figure 2. The KBR topological graph.

[N], [B] and [C], respectively, represent the column matrix representing the nodes, the column matrix representing the branches and the incidence matrix branches/nodes. The incidence matrix allows the transition from the variables associated with the nodes to the variables associated with the branches: the lines correspond to the branches and the columns correspond to the nodes. The coefficients of the incidence matrix indicate:

$$C(i,j) = \begin{cases} 1 & \text{if } P_i \text{ is an input node} \\ -1 & \text{if } P_i \text{ is an output node} \\ 0 & \text{else} \end{cases}$$

[Y] and [Z], respectively, represent the admittance and impedance matrices. They allow the expression of the geometrical and physical relationships that occur between the elements of the primal and dual objects (e.g. of primal/dual object: force/displacement, Voltage/current …). The existence of [Z_N] is subject to the condition that [Y_N] is invertible.

The topological graph KBR creates interesting perspectives for the modelling of mechanical or mecatronic systems, particularly, when the same representation leads to different modelling. Therefore, based on the converse analogy (Firestone, 1933), the KBR topological graph can be used as a unification basis for the modelling of multi-physics systems.

For example, we consider the linear graph presented in Figure 3. This graph is composed of two nodes noted P_1 and P_2 and one arc noted e_1 and it is oriented from P_1 to P_2. The incidence matrix associated with this graph is $[C] = [1 - 1]$. Based on the converse analogy, this graph can present a tension spring in the mechanical field or an electric resistance in the electrical field.

For the tension spring, we associate the displacement vector with the nodes $\begin{Bmatrix} dx_1 \\ dx_2 \end{Bmatrix}$. The incidence matrix applied to the nodes provides the displacement of the spring $\Delta l = dx_1 - dx_2$. The transition to the dual spaces corresponds to the forces associated with the nodes $\begin{Bmatrix} F_1 \\ F_2 \end{Bmatrix}$ and the arc F. This transition is done using the admittance matrix $[Y] = [k]$ that allows the expression of the behaviour law of the spring $F = k\Delta l$.

For the electric resistance, we associate the voltage vector with the nodes $\begin{Bmatrix} V_1 \\ V_2 \end{Bmatrix}$. The incidence matrix applied to the nodes provides the voltage of the resistance $U = V_1 - V_2$. The transition to the dual spaces corresponds to current associated with the nodes $\begin{Bmatrix} I_1 \\ I_2 \end{Bmatrix}$ and the arc I. This transition is done using the admittance matrix $[Y] = [1/R]$ that allows the expression of the behaviour law of the electric resistance $I = (1/R)U$.

2.2. MGS language: Topological collections and transformations

As a language allowing the application of the KBR topological graph, we used the MGS that embedded the concept of topological collections and their transformations into the framework of a simple dynamically typed functional language.

A topological collection is a collection in which the structure is captured by a neighbourhood relationship among the data. In other words, from providing one of the

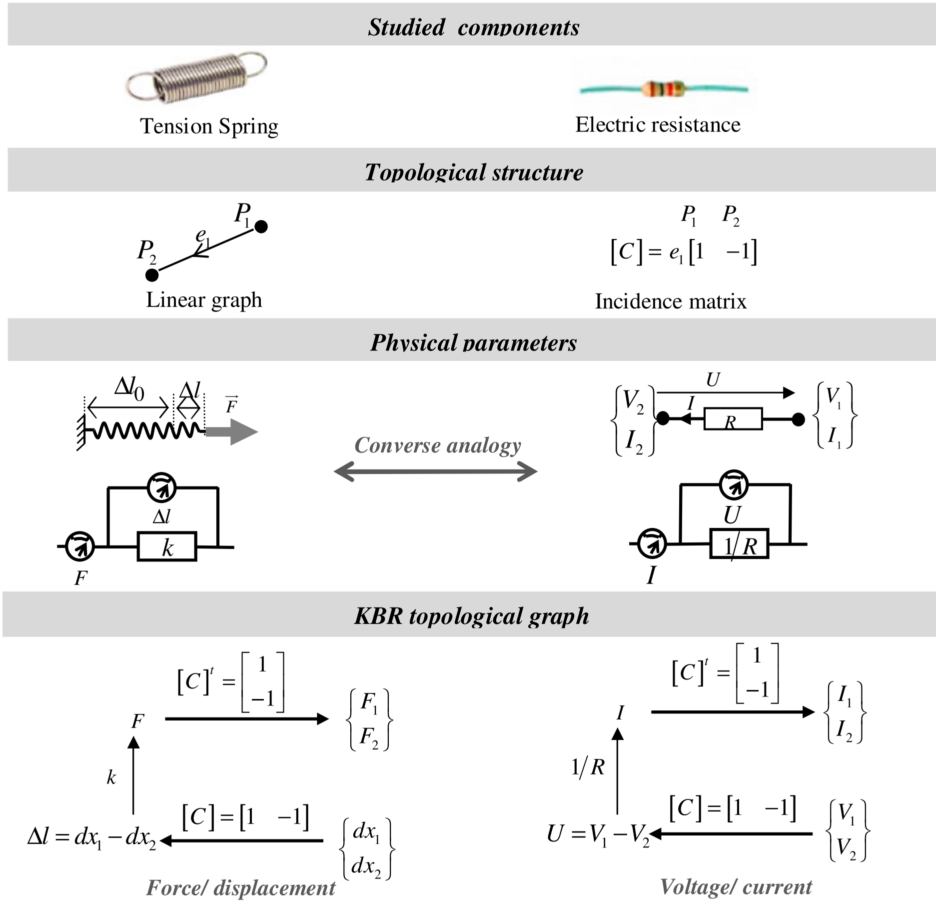

Figure 3. The KBR topological graph based on the converse analogy in the case of a tension spring and an electric resistance.

elements in the collection, we can provide all the other data that are directly related. The organisation of a topological collection is founded on a cellular complex, where the values are associated with each cell. A cellular complex is made of elements of various dimensions called topological cells of dimension n or n-cells (0-cells represent vertices, 1-cells represent edges, 2-cells represent faces …). These basic elements are organised following the incidence relationship that relies on the notion of boundary: let c_1 and c_2 be, respectively, an n_1 -cell and an n_2 -cell with $n_1 \langle n_2$, if $n_1 = n_2 - 1$, c_1 is called a face of c_2, and c_2 is a co-face of c_1.

Transformations (paths, functions defined by case, patches …) are functions operating on the topological collections. They are defined by a set of rewritten rules of the form $m \Rightarrow e$. The left-hand part of the rule is called pattern and the right-hand part is the expression that replaces the instances of m.

The application of a transformation to a collection is as follows: a number of non-intersecting occurrences of the first pattern are selected and then replaced with the appropriate element calculated from the corresponding expression. When we cannot find a new instance of the first pattern, we select a number of non-intersecting occurrences of the second pattern among the elements that haven't been selected yet, and so on. When this process is finished, we replace the selected elements by the new corresponding elements and the new collection is thus created.

3. A case study: piezoelectric structure

3.1. Theory of piezoelectric structure

3.1.1. Piezoelectric converse and direct effect

Piezoelectricity is the property of some materials that become electrically charged, when subjected to a mechanical stress. This behaviour, which is spontaneous, is due to the crystal structure. Indeed, when a mechanical action is applied to a piezoelectric volume, an electric dipole appears in each crystal unit cell due to the displacement of the centres of the positive and negative charges. Electrostatic balance being broken, a polarisation appears: this is the piezoelectric direct effect as shown in Figure 4(a). There is also a converse effect: a piezoelectric material subjected to an electric field undergoes a mechanical deformation as illustrated in Figure 4(b).

3.1.2. Piezoelectric equations

For linear piezoelectric materials simultaneously submitted to a mechanical deformation process and an electrical polarisation process, the constitutive equations are written in matrix form as follows (IEEE standard of piezoelectricity, 1988):

$$\begin{cases} \{\sigma\} = [c^E]\{\varepsilon\} - [e]^T\{E\} \\ \{D\} = [e]\{\varepsilon\} - [\in^S]\{E\} \end{cases} \tag{1}$$

where $\{\sigma\} = \{\sigma_{11}\sigma_{22}\sigma_{33}\sigma_{23}\sigma_{13}\sigma_{12}\}$: Stress vector $\mathrm{N/m^2}$, $\{\varepsilon\} = \{\varepsilon_{11}\varepsilon_{22}\varepsilon_{33}\varepsilon_{23}\varepsilon_{13}\varepsilon_{12}\}$: Strain vector (m/m), $\{E\} = \{E_1E_2E_3\}$: Vector of applied electric field (V/m), $\{D\} = \{D_1D_2D_3\}$: Vector of electric displacement ($\mathrm{C/m^2}$) $[c^E]$: Mechanical stiffness matrix for a constant electric field (Pa), $[e]$: Piezoelectric coupling coefficients matrix (N/m/V), $[e]^T$ is the transposed, $[\in^S]$: Dielectric constant matrix for constant mechanical strain (F/m).

3.1.3. The main piezoelectric coupling modes

There are various vibration modes of a piezoelectric structure. Figure 5 illustrates the main coupling modes in the case of a rectangular bar of a piezoelectric ceramic. In

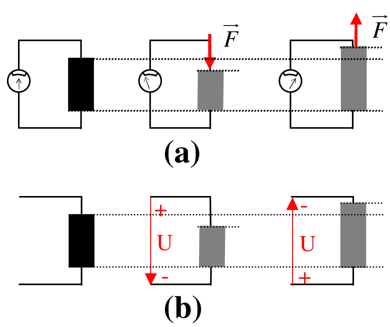

Figure 4. Piezoelectric effect. (a) Direct piezoelectric effect, (b) Converse piezoelectric effect.

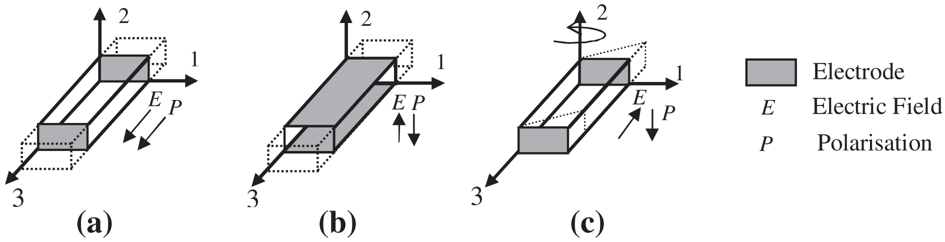

Figure 5. The different coupling modes of a rectangular piezoelectric bar (a) The longitudinal mode (b) The transverse mode (c) The shear mode.

general, a piezoelectric ceramic is referenced by a Cartesian reference triad (O, x_1, x_2, x_3). Conventionally, the displacement and the direction of polarisation are coincident with the axis 3.

- The longitudinal mode (mode 33) results in a change in length along the axis 3, when an electric field is applied along the same axis by means of electrodes placed on the sides perpendicular to this axis,
- The transverse mode (mode 31 or 32) leads to a change in length along the axis 3, when an electric field is applied along the axis 2 or 1,
- The shear mode (mode 15) leads to shear deformation around the axis 2, when an electric field is applied along the axis 3.

The longitudinal mode is the most interesting in terms of coupling and should be favoured whenever it is possible.

3.2. Example 1: Multi layer piezoelectric stack

3.2.1. Description

Multi layer piezoelectric stack is obtained by a stack of piezoelectric ceramic isolated from each other but electrically connected in parallel in an adequate armature. The polarisation direction of each element is parallel to the direction in which the elongation and/or the force must be developed (Figure 6(a)).

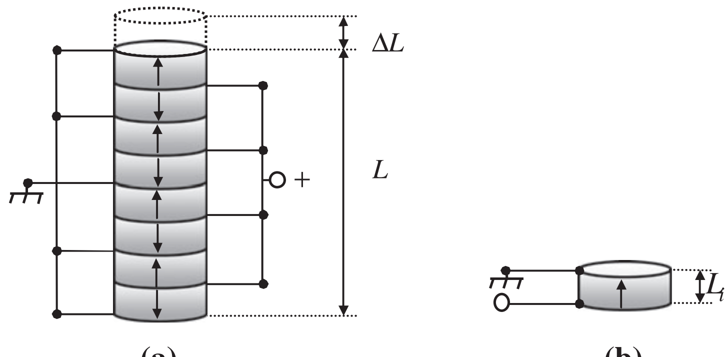

Figure 6. (a) Multi layer piezoelectric stack (b) Piezoelectric stack element.

When we apply a voltage U across the electrodes, each piezoelectric stack element lies down along the polarisation direction. That is to say, we are interested in mode 33. Then, the behaviour law for a piezoelectric stack element can be written in a matrix form as follows:

$$\begin{pmatrix} \sigma_{3i} \\ D_{3i} \end{pmatrix} = \begin{bmatrix} C_{33i}^E & -e_{33i} \\ e_{33i} & \in_{33i} \end{bmatrix} \begin{pmatrix} \varepsilon_{3i} \\ E_{3i} \end{pmatrix} \tag{2}$$

where $i = 0 \ldots n$ and n is the number of the piezoelectric stack element.

For small deformations, the electric field vector E_{3i} can be simply expressed as a function of U_i:

$E_{3i} = U_i/Li$, where L_i presents the length of a piezoelectric stack element.

We assume a static regime, that is to say that changes in external forces F_i to the piezoelectric stack element are practically null, and so the dynamic effects are neglected. Then, the vector stress is given by the following:

$F_i = \int\int_{Ai} \sigma_{3i} dA_i = \sigma_{3i} A_i \Longrightarrow \sigma_{3i} = F_i/A_i$, where A_i is the cross-sectional area of the piezoelectric stack element.

The electric charge in a piezoelectric element is given by $Q_i = \int\int_{Ai} D_{3i} dA_i = D_{3i} A_i$

On the other hand, $I_i = dQ_i/dt$ then $I_i = d(A_i D_{3i})/dt = p A_i D_{3i}$ (Where p is the Laplace variable)

Thus, we can write the piezoelectric behaviour law for a piezoelectric stack element as follows:

$$\begin{pmatrix} I_i \\ F_i \end{pmatrix} = \begin{bmatrix} (pA_i)/L_i & 0 \\ 0 & A_i/L_i \end{bmatrix} \begin{bmatrix} \in_{33i} & e_{33i} \\ -e_{33i} & C_{33i}^E \end{bmatrix} \begin{pmatrix} \Delta U_i \\ \Delta L_i \end{pmatrix} \tag{3}$$

We note: $[K]_{piezi} = \begin{bmatrix} (pA_i)/L_i & 0 \\ 0 & A_i/L_i \end{bmatrix} \begin{bmatrix} \in_{33i} & e_{33i} \\ -e_{33i} & C_{33i}^E \end{bmatrix}$

3.2.2. Topological graph KBR

3.2.2.1. For a piezoelectric stack element. The linear graph corresponding to a piezoelectric stack element is shown in Figure 7. The incidence matrix associated with this graph is as follows: $[C] = [1 - 1]$.

For this topological structure the vector $\{\overrightarrow{\Delta P_{P_i}}\}_{piez} = \begin{Bmatrix} Z_{P_i} \\ V_{P_i} \end{Bmatrix}$; $i = 1, 2$ is associated with the nodes where Z_i and V_i, respectively, represent the displacement along the Z axis and voltage of the node $P_i\,(i = 1, 2)$. The incidence matrix applied to these nodes provides the voltage $V_{e_1} = V_1 - V_2$ and the displacement $Z_{e_1} = Z_{P_1} - Z_{P_2}$ of the

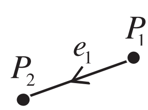

Figure 7. Linear graph of a piezoelectric stack element.

piezoelectric stack element $\{\Delta e_1\}_{piez} = \begin{Bmatrix} V_{e1} \\ Z_{e1} \end{Bmatrix}$. The transition to the dual space corresponds to the force and the current associated with the nodes and the arc $\{\overrightarrow{\tau_{e_1}}\}_{piez} = \begin{Bmatrix} I_{e_1} \\ F_{e_1} \end{Bmatrix}$. By adding the behaviour law linking the two dual spaces (equation (3)), we obtain the KBR topological graph for a piezoelectric stack element (Figure 8).

3.2.2.2. For a piezoelectric stack with n elements. The linear graph corresponding to a multi layer piezoelectric stack with n piezoelectric stack element is made up by $n+1$ nodes and n arcs (Figure 9(a)). The incidence matrix associated with this graph is given in Figure 9(b).

Relying on the KBR topological graph of a piezoelectric stack element, we determine the one corresponding to the piezoelectric stack with n elements (Figure 10).

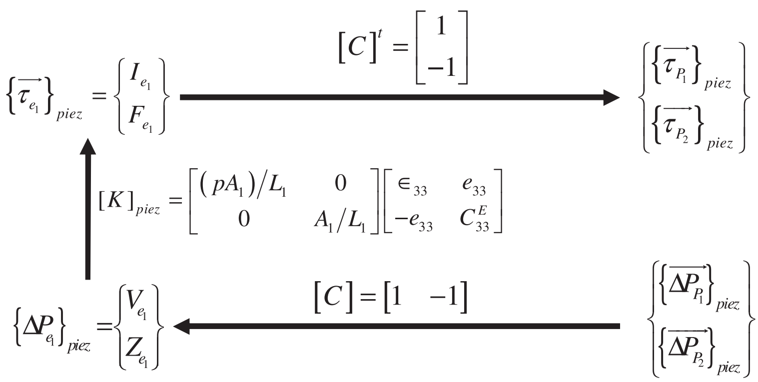

Figure 8. KBR topological graph for a piezoelectric stack element.

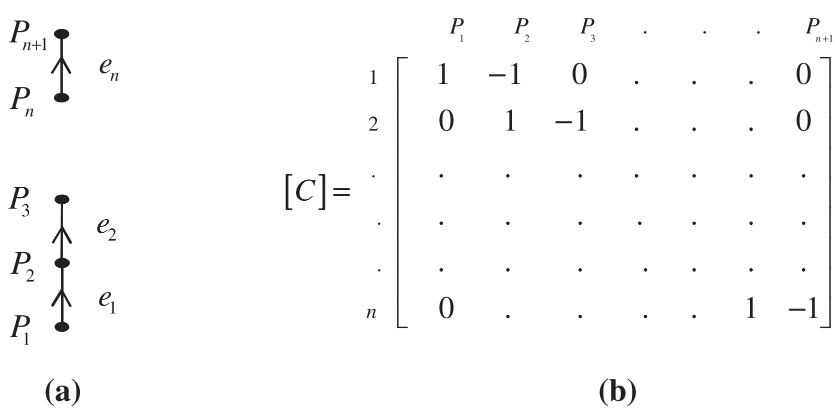

Figure 9. Multi layer piezoelectric stack (a) linear graph (b) incidence matrix.

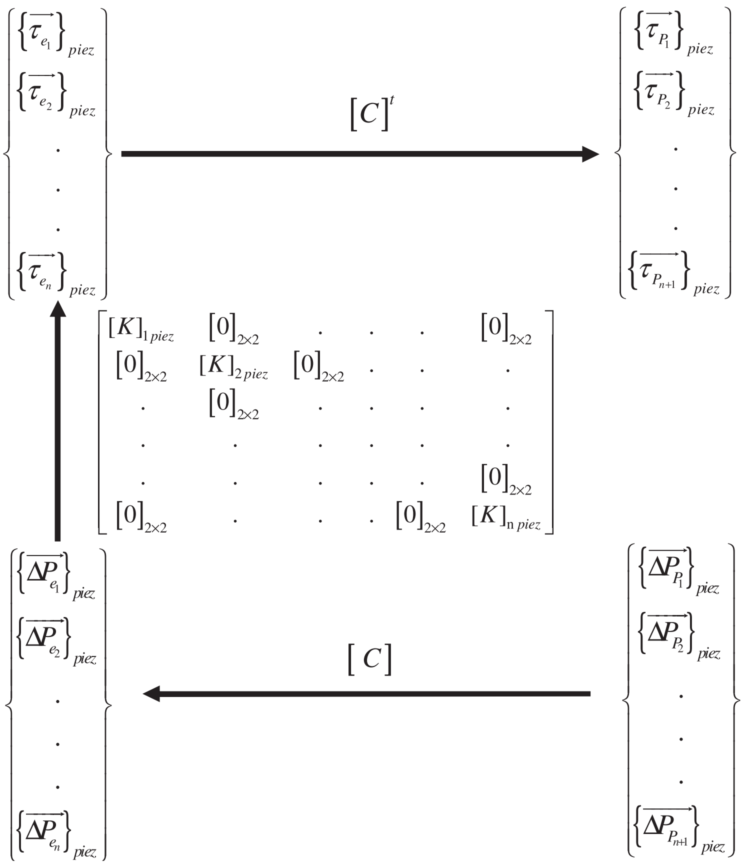

Figure 10. KBR topological graph for a piezoelectric stack with n elements.

3.2.3. MGS Modelling

3.2.3.1. For a piezoelectric stack element. First, we begin with the definition of the cells representing the piezoelectric stack element. We use only cells of dimensions 0 and 1.

- 0-cells represent the nodes noted P_1 and P_2.
- 1-cells can represent:

  (a) The piezoelectric stack element noted e_{p1}
  (b) The two electrical grounds noted e_{m1} and e_{m2} (the two nodes are connected to the electrical ground)
  (c) The frame noted e_{b1}

The 1-cells representing the piezoelectric stack element differ from those representing the frame and the electrical ground in that they are bounded by two nodes. Then, we define the functions of the piezoelectric variables and, we associate them with the corresponding k-cells. Finally, we generate the system of equations of the piezoelectric stack elements, taking into account that this system should be written in a format that is executable by other software. In our case, the equations are written in MODELICA format, and we use Dymola as a solver. The generation of the system of equations is done by sweeping all the cells and by defining the local behaviour law of each cell.

- For 0-cells, we have $\sum_{j=1}^{N} \overrightarrow{F_j} = \overrightarrow{0}$ and / or $\sum_{j=1}^{N} I_j = 0$ Where $\overrightarrow{F_j}$ and I_j, respectively, represent the normal force and the electric current of each arc connected to the isolated node and N the number of concurrent arcs to the node.
- For 1-cells, they can present (i and j denote the ends of the arc)

  (a) The piezoelectric stack element in this case, we have $\begin{cases} \overrightarrow{F_i} + \overrightarrow{F_j} = \overrightarrow{0} \\ I_i + I_j = 0 \\ \overrightarrow{\Delta P_{piez}} = [K]_{piez} \overrightarrow{\tau_{piez\_e}} \end{cases}$

  (b) The frame, in this case, we have $\overrightarrow{F_i} + \overrightarrow{F_j} = \overrightarrow{0}$

  (c) The electrical ground, in this case we have $I_i + I_j = 0$

3.2.3.2. For a multilayer piezoelectric stack. The modelling steps are the same as a piezoelectric stack element (Figure 11). The only difference is at the level of the declaration of the cells representing the studied multilayer piezoelectric stack because this step depends on the number of the stack elements (topological structure).

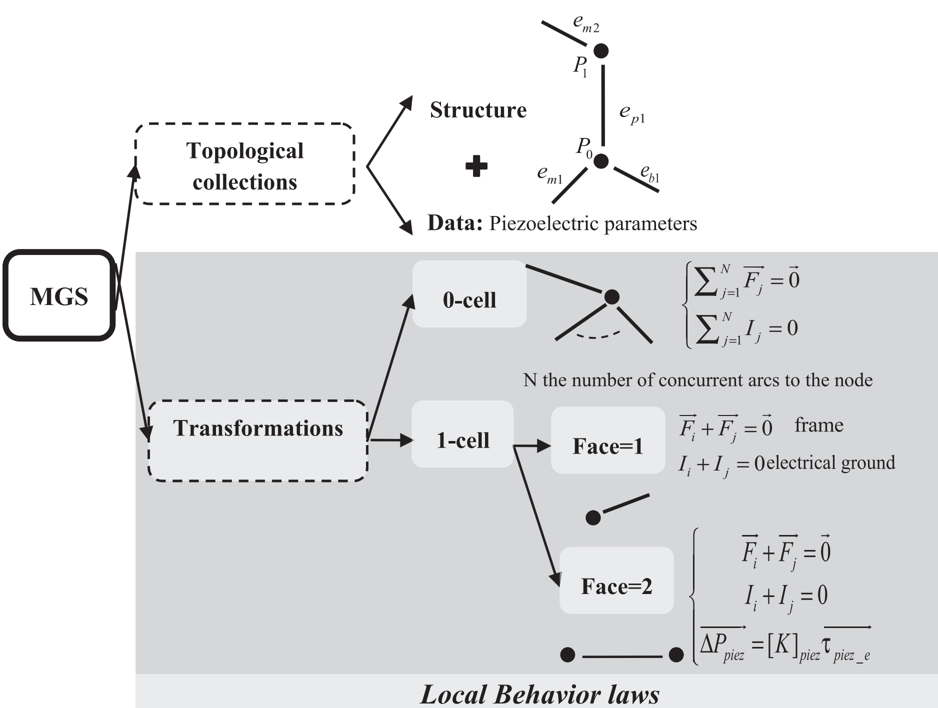

Figure 11. Modeling principal steps of a piezoelectric stack element using MGS language.

3.2.4. A Particular case and numerical results

Considering a simple case of a piezoelectric stack consisting of three-layers of thickness $e = 0.02\,\mathrm{m}$ and section $A = 0.25\mathrm{E} - 5\,\mathrm{m}^2$. The piezoelectric material properties are (Boucher, Lagier, & Maerfeld, 1981): $C_{33}^{E} = 11.5\ 10^{10}\mathrm{N/m}^2$, $e_{33} = 14.1\ \mathrm{C/m}^2$ $\in_{33} = 5.838345\,10^{-9}\,\mathrm{F/m}$.

In order to validate the results obtained using the concept of topological collections and transformations, we compare the results obtained by the MGS language and those obtained by ANSYS. SOLID 5 is taken from the ANSYS library as a finite element. The nodes of this element have six degrees of freedom which are the displacements along the axes *x, y, z*, the intensity of the electric potential, the intensity of the magnetic field and temperature. So this is a multi-field element. Since we are discussing the linear piezoelectricity, the displacements and electric potential are of interest for us.

Tables 1 and 2 show the different results using the MGS as well as those obtained by ANSYS for $U = 1000\,V$.

The results obtained by the MGS language based on topological collections and transformations are very close to those obtained by the ANSYS software based on the finite element method.

We can also notice that the total elongation of the piezoelectric stack is equal to $3 \times 0.12261E - 06$.

Where 3 represents the number of the piezoelectric elements and $0.12261E - 06$ represents the elongation of one of the piezoelectric stack element.

Indeed, we can write the behaviour law of a piezoelectric stack consisting of n piezoelectric elements having the same physical and geometrical properties as follows:

$$\begin{pmatrix} I_{stack} \\ F_{stack} \end{pmatrix} = \begin{bmatrix} (pA)/L & 0 \\ 0 & A/L \end{bmatrix} \begin{bmatrix} n \in_{33} & e_{33} \\ -e_{33} & (1/n)C_{33}^{E} \end{bmatrix} \begin{pmatrix} \Delta U_{stack} \\ \Delta L_{stack} \end{pmatrix} \tag{4}$$

We note: $[K]_{stack} = \begin{bmatrix} (pA)/L & 0 \\ 0 & A/L \end{bmatrix} \begin{bmatrix} n \in_{33} & e_{33} \\ -e_{33} & (1/n)C_{33}^{E} \end{bmatrix}$

where A and L, respectively, represent the cross-sectional area and length of a piezoelectric stack element and n the number of the piezoelectric stack elements.

Table 1. Electric current at the arcs (A).

	MGS	ANSYS
e_1	.946236E−08	.946236E−08
e_2	.946236E−08	.946236E−08
e_3	.946236E−08	.946236E−08

Table 2. Displacement of the nodes (m).

	MGS	ANSYS
P_1	0	0
P_2	−.122609E−06	−.12261E−06
P_3	−.245217E−06	−.24522E−06
P_4	−.367826E−06	−.36783E−06

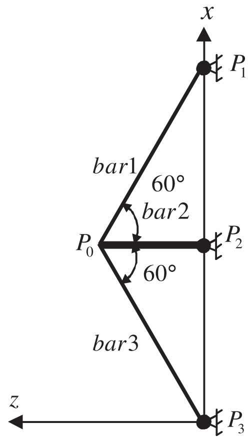

Figure 12. The three-bar piezoelectric truss.

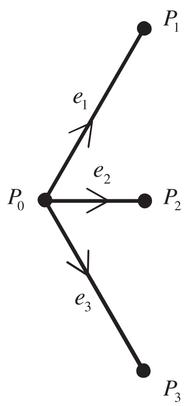

(a)

$$[C] = \begin{array}{c} \\ e_1 \\ e_2 \\ e_3 \end{array} \begin{array}{c} \begin{array}{cccc} P_0 & P_1 & P_2 & P_3 \end{array} \\ \begin{bmatrix} 1 & -1 & 0 & 0 \\ 1 & 0 & -1 & 0 \\ 1 & 0 & 0 & -1 \end{bmatrix} \end{array}$$

(b)

Figure 13. The three-bar piezoelectric truss (a) linear graph (b) incidence matrix.

3.3. Example 2:Planar piezoelectric truss structure

3.3.1. Description

We consider a two-dimensional three bar truss structure articulated to a rigid support in P_1, P_2 and P_3 as shown in Figure 12. This truss has only one piezoelectric bar which is bar 2. We consider that the piezoelectric bar is a multi-layer piezoelectric stack having the same geometrical and physical properties of the one used in the previous example.

3.3.2. KBR topological graph

The linear graph corresponding to *the three-bar piezoelectric truss* element is made up by 4 nodes and 3 arcs (Figure 13(a)). The incidence matrix associated with this graph is given in Figure 13(b).

After determining the KBR topological graph for a bar element in tension/compression (Miladi Chaabane et al., 2012) (Figure 14(b)) and that of a multilayer piezoelectric stack (Figure 14(a)), we determine the KBR topological graph for the three-bar piezoelectric truss given in Figure 14(c).

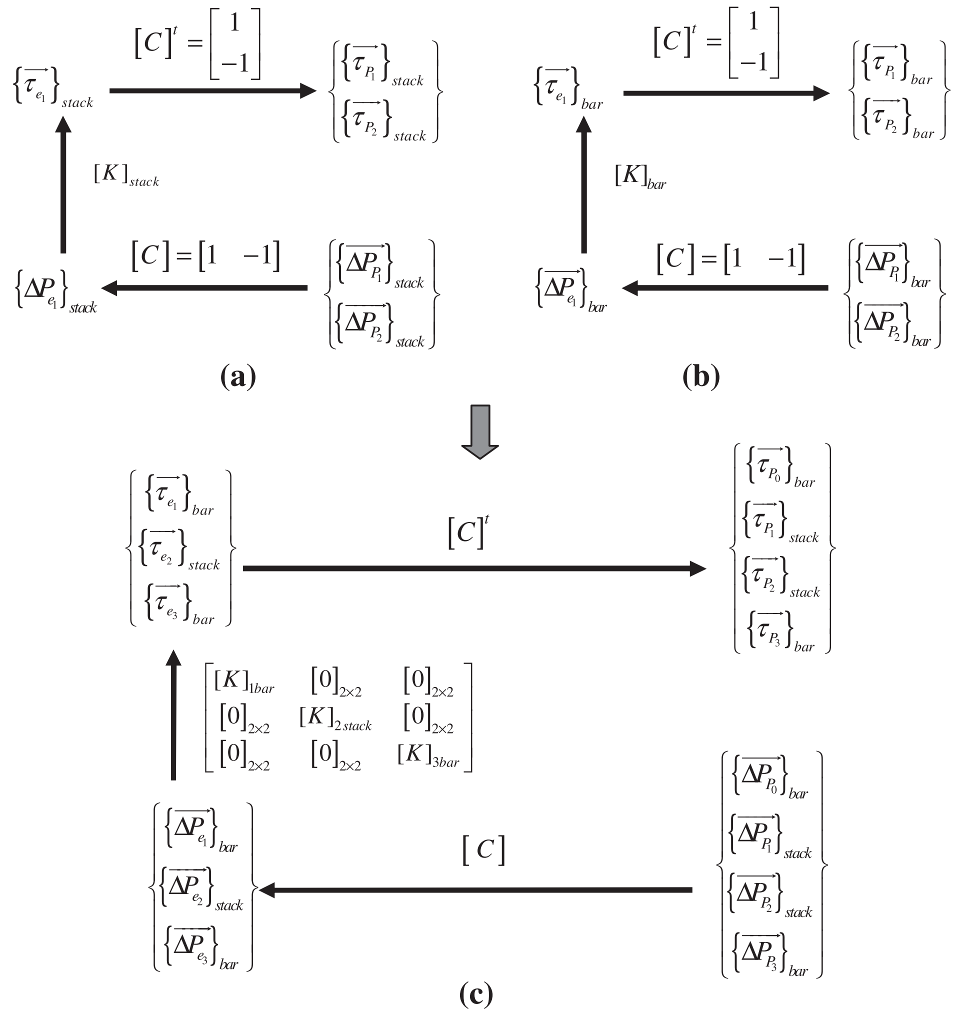

Figure 14. KBR topological graph of the three-bar piezoelectric truss.

3.3.3. MGS Modelling

The modelling steps of the three-bar piezoelectric truss are presented in Figure 15. First, we begin with the definition of the cells representing the piezoelectric truss structure.

- 0-cells represent the nodes noted P_0, P_1, P_2 and P_3.
- 1-cells can represent:

  (a) The piezoelectric bar noted e_{p2}
  (b) The two bars noted e_1 and e_3
  (c) The two electrical ground noted e_{m1} and e_{m2} (the two nodes P_0 and P_2 are linked to the electrical ground)
  (d) The three frames noted e_{b1}, e_{b2} and e_{b3} (the three nodes P_1, P_2 and P_3 are linked to a rigid support).

Then, in addition to the function of the piezoelectric variables, we add the function of the mechanical variables and we associate them to the corresponding k-cells. Finally, we generate the system of equations of the piezoelectric stack element, taking into account that the latter should be written in a format executable by other software. In our case, the equations are written in MODELICA format, and we use Dymola as a solver. The generation of the system of equations is done by sweeping all the cells and defining the local behaviour law of each cell. Compared with the piezoelectric stack, we add the local behaviour law for a bar element (Miladi Chaabane et al., 2012): $\begin{cases} \overrightarrow{F_i} + \overrightarrow{F_j} = \overrightarrow{0} \\ \overrightarrow{\Delta P} = [K]_{bar} \overrightarrow{\tau_e} \end{cases}$ Where $[K]_{bar} = [(EA)/L] \begin{bmatrix} c^2 & cs \\ cs & s^2 \end{bmatrix}$ (L: length of the bar, A: the cross-sectional area of the bar, E: the Young's modulus of the bar, $c = \cos(\theta);\ s = \sin(\theta)$).

3.3.4. Numerical results

The two bars noted bar 1 and bar 3 are identical:

Young's modulus: $E_1 = E_3 = 200\,\text{GPa}$, cross sectional area: $A_1 = A_3 = 2.5E - 5\text{m}^2$ and length $L_1 = L_3 = 0.12\text{m}$.

For the piezoelectric bar, we have the same geometrical and physical parameters of the piezoelectric stack previously used.

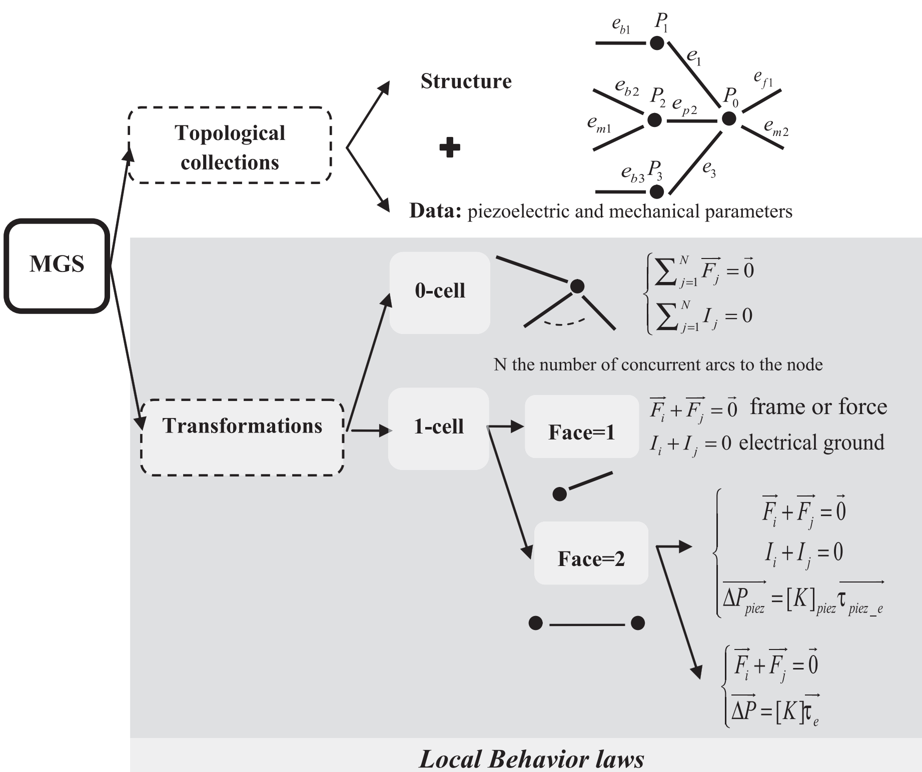

Figure 15. Modeling principal steps of the three-bar piezoelectric truss structure using the MGS language.

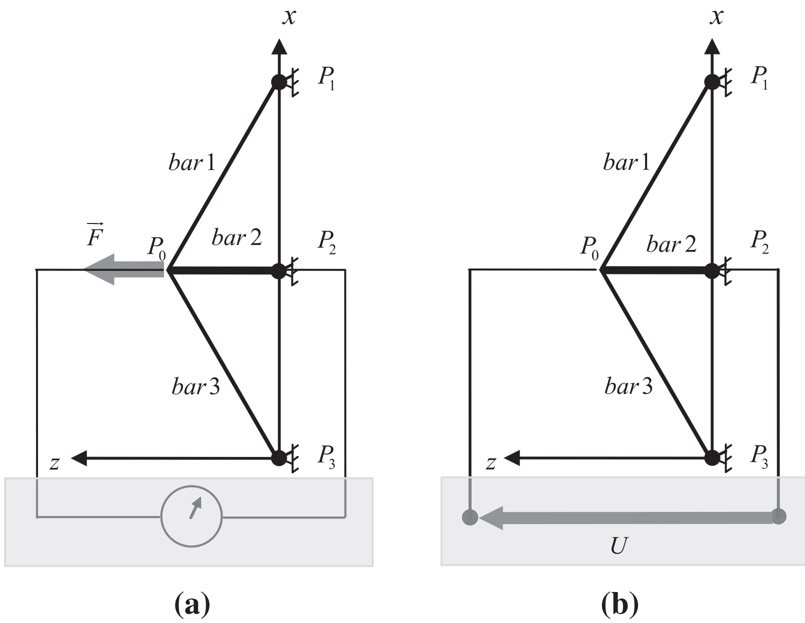

Figure 16. Piezoelectric effect of the three-bar piezoelectric truss (a) Direct piezoelectric effect (b) Converse piezoelectric effect.

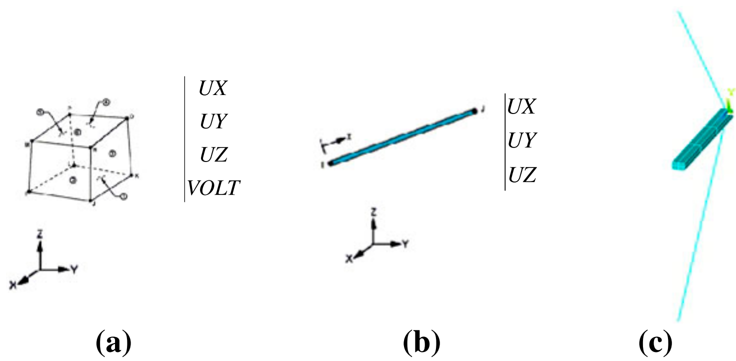

Figure 17. (a) SOLID5 Geometry (b) LINK8 Geometry (c) Three-bar piezoelectric truss structure.

Table 3. Electric current at the piezoelectric stack (A).

	MGS	ANSYS
bar_2	.2635443E−7	.2635428E−07

We studied the direct piezoelectric effect and the converse piezoelectric effect.

- The direct piezoelectric effect: the truss is subjected to a force $F = 1000N$ applied to the node P_0. This force implies a deformation of the three bars. Then, the piezoelectric bar is an electrically polarised (Figure 16(a)).

- The converse piezoelectric effect: the truss is not subject to any external force. The piezoelectric bar is subjected to a voltage $U = 1000\,V$ (Figure 16(b)).

In order to validate the results obtained using the concept of topological collections and transformations, we compare the results obtained by the MGS language to those obtained by ANSYS. As a finite element, from the library of ANSYS, the element SOLID 5 is taken for the piezoelectric bar 2, and LINK 8 is taken for the two bars noted bar 1 and bar 3 (Figure 17).

- For the converse piezoelectric effect ($U = 1000\,V$): Tables 3–5, respectively, represent the electric current at the piezoelectric stack, the displacement of the node P_0 along the z direction and the support reactions obtained using the MGS language as well as those obtained by the software of the finite element method ANSYS.

Table 4. Displacement of the node P_0 (m) along the z direction.

	MGS	ANSYS
P_0	.252498E−6	.25250–6

Table 5. Support reactions (N).

	MGS	ANSYS
P_1	[4.78472 2.76307]	[4.7847 2.7631]
P_2	[0 − 5.52615]	[.177639E − 14 − 5.5261]
P_3	[−4.78472 2.76307]	[−4.7847 2.7631]

Table 6. Electric current at the piezoelectric stack (A).

	MGS	ANSYS
bar_2	.252498−06	.2524998E−06

Table 7. Displacement of the node P_0 (m) along the z direction.

	ANSYS	MGS
P_0	.143261E−4	.14326E−4

Table 8. Support reactions (N).

	MGS	ANSYS
P_1	[271.474 −156.77]	[271.47 −156.77]
P_2	[0 −686.46]	[.156323E−12 −686.46]
P_3	[−271.474 −156.77]	[−271.47 −156.77]

- For the direct piezoelectric effect ($F = 1000\,N$): Tables 6–8, respectively, represent the electric current at the piezoelectric stack, the Displacement of the node P_0 along the z direction and the support reactions obtained using the MGS language as well as those obtained by the software of the finite element method ANSYS.

The results obtained by the MGS language based on topological collections and transformations are very close to those obtained by the software ANSYS based on the finite element method.

4. Conclusion

In this study, we presented a new topological approach for the modelling of mecatronic systems on the basis of topological collections and transformations. This approach was applied in the case of piezoelectric actuator stack and the case of piezoelectric truss structure. The results are validated using the software of the finite element analysis ANSYS.

The major advantage of this approach is the separation of the topology (interconnection law) and the behaviour laws (physics) of the studied system, which allows the formation of generic models. Therefore, we can create an MGS library by defining the local behaviour laws of the different fields of mecatronics.

The perspective of this study is the application of this topological approach for the modelling of more complex systems (multi-physics: mechanical, electrical, hydraulic, thermal …).

References

Björke, Ø. (1995). *Manufacturing systems theory – A geometric approach to connection*. Trondheim- Norway: Tapir.

Boucher, D., Lagier, M., & Maerfeld, C. (1981). Computation of the vibration modes for piezoelectric array transducers using a mixed finite element perturbation method. *IEEE Transactions Sonics and Ultrasonics, 28*, 318–330.

Branin, F. H. Jr. (1966). The algebraic topological basis for network analogies and the vector calculus. In *Proceedings of the Symposium on Generalized Networks, 16*, 453–491.

Cohen, J. (2004). *Intégration des collections topologiques et des transformations dans un langage fonctionnel*. PhD thesis, University of Evry Val d'Essonne.

Egli, R. (2000). *Cadre de travail pour la spécification de systèmes avec des chaînes sur un complexe cellulaire*. PhD thesis, *University of Montreal*.

Firestone, F. (1933). A new analogy between mechanical and electrical systems. *Journal of the Acoustical Society of America, 4*, 249–267.

Giavitto, J.-L., Godin, C., Michel, O., Prusinkiewicz, P. (2002). *Modelling and Simulation of biological process in the context of genomics*, chapter *Computational Models for Integrative and Developmental Biology*. Hermes.

IEEE. (1988). *IEEE standard on piezoelectricity*. New York, NY: Institute of Electrical and Electronics Engineers.

Kron, G. (1942). *A short course in tensor analysis for electrical engineers*. Wiley New York London: Chapman & Hall.

Kron, G. (1963). *Diakoptics; The Piecewise Solution for Large-Scale System*. London: Macdonald.

Miladi Chaabane, M., Plateaux, R., Choley, J.-Y., Karra, C., Riviere, A., & Haddar, M. (2012). Topological approach to solve 2D truss structure using MGS language. *IEEE MECATRONIC REM,* 437–444. doi:10.1109/MECATRONICS.2012.6451045

MODELICA. *Modeling of Complex Physical Systems*. Retrieved February 2013, from http://www.modelica.org

Plateaux, R. (2011). *Continuité et cohérence d'une modélisation des systèmes mécatroniques basée(s) sur une structure topologique*. PhD thesis, Superior Engineering Institute of Paris SUPMECA.

Plateaux, R., Penas, O., Rivière, A., Choley, J-Y. (2007). Need for the definition of a topological structure for the complex systems modeling. CPI 2007.

Roth, J.-P. (1955). An application of algebraic topology to numerical analysis: On the existence of a solution to the network problem. *Proceedings of the National Academy of Sciences, 41*, 518–521.

Shai, O. (2001a). Combinatorial representations in structural analysis. *Computing in Civil Engineering, 15*, 193–207.

Shai, O. (2001b). Deriving structural theorems and methods using tellegen's theorem and combinatorial. *International Journal of Solids and Structures, 38*, 8037–8052.

Shai, O. (2001c). The multidisciplinary combinatorial approach and its applications in engineering. *AIEDAM - AI for Engineering Design, Analysis and Manufacturing, 15*, 109–144.

Spicher, A. (2006). *Transformation de collections topologiques de dimension arbitraire. Application* à la *modélisation de systèmes dynamiques*, PhD thesis, University of Evry.

Spicher, A., & Michel, O. (2007). Declarative modeling of a neurulation-like process. *BioSystems, 87*, 281–288.

The MGS home page. Retrieved February 2013, from http://www.ibisc.univ-evry.fr/~mgs/

Tonti, E. (2003). *A Classification Diagram for Physical Variables* (draft). Retrieved February 2013, from http://www.dic.units.it/perspage/discretephysics/papers/diagrammi.pdf